# The evolution of interferometry from metrology to biomedical applications

James C. Wyant
College of Optical Sciences, University of Arizona, 1630 E. University Blvd., Tucson, AZ, USA 85721-0094

## ABSTRACT

Interferometry is a powerful tool often used for the metrology of surfaces with many applications in industries such as optical fabrication, data storage, machine tool, and semiconductor. For many years interferometers have been built into microscopes so surface microstructure can be measured. Phase-shifting interferometric techniques have provided an extremely accurate rapid way of getting the interferogram data into the computer and the inherent noise in the data taking process is so low that in a good environment angstrom or sub-angstrom surface height or thickness measurements can be performed. The recent development of single-shot phase-shifting techniques has made it possible to perform accurate phase measurement techniques in less than ideal environments and to make movies showing how surface shape or optical thickness is varying with time. These same interferometric techniques can be applied to biomedical applications. This paper will trace the history of the development of these interferometric techniques that led to the application of these techniques to looking at cells and tissues.

**Keywords:** phase measurement, interferometry, phase-shifting, metrology, interferometric, optical measurement, interferometric microscope, phase imaging

## 1. INTRODUCTION

Interferometry is an extremely powerful tool for measuring surface height or optical thickness variations of samples with applications in many, many fields. To make interferometry most useful, it is essential that there is a good way of getting the interferometric data into the computer so this interferometric data can be analyzed to get the most information possible about the sample being measured or studied. Since the personal computer has become readily available in the 1980s many techniques have been developed for getting interferometric data into a computer. The purpose of this paper is to briefly look at many of the best techniques. While most of these techniques were developed for applications in metrology, these same techniques can be applied for looking at cells and tissues.

The paper begins with a brief look at basic interferometry and two basic interferometers. This will be followed by a description of phase-shifting interferometry, vertical scanning interferometry, and various single-shot dynamic interferometry approaches for rapidly getting interferometric data into the computer. Throughout the paper metrology applications will be illustrated. The paper will conclude with a brief introduction to using these interferometric phase gathering techniques in biomedical/biological applications.

## 2. BASIC INTERFERENCE AND INTERFEROMETRY

Interference and interferometry are described in many, many references.[1-6] As far as this paper is concerned we will be involved only with two-beam interference and we will assume the two beams are coherent with respect to each other so when the two beams are combined interference fringes will be obtained as shown in Figure 1. If the wavefronts of the two interfering beams match, except for a tilt between the two beams, straight equally-spaced fringes result. As shown below, the shape and deviation from equal spacing of the fringes gives the phase difference between the two interfering beams. The well know two-beam equation below describes the irradiance of the interference pattern. $I_1$ and $I_2$ are the irradiances of the two interfering beams and $\emptyset_1 - \emptyset_2$ is the phase difference between the two interfering beams.

$$I = I_1 + I_2 + 2\sqrt{I_1 I_2}\cos(\emptyset_1 - \emptyset_2)$$

Quantitative Phase Imaging II, edited by Gabriel Popescu, YongKeun Park, Proc. of SPIE Vol. 9718, 971802

We can write the phase difference as

$$\emptyset_1 - \emptyset_2 = \left(\frac{2\pi}{\lambda}\right)(\text{optical path difference})$$

There may also be a term due to phase changes upon reflection, but in the majority of applications we can neglect this phase change. Thus, in most cases we are measuring the optical path difference (OPD). If we are looking at a surface at normal incidence the OPD is given by 2 times the height variations of the sample being measured. If we are looking at a sample in transmission, we are measuring the refractive index minus one times the thickness variations of the sample times. That is,

$$\text{OPD} = (\text{n} - 1)(\text{Thickness Variation})$$

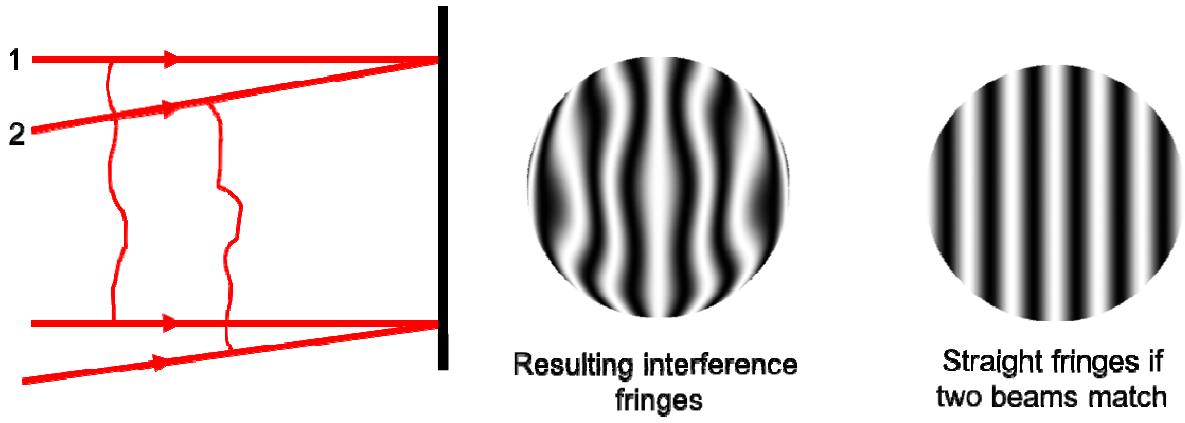


Figure 1. Interference of two beams of light.

It is important to remember that if we are measuring the sample in double pass, the OPD increases by a factor of two.

There are hundreds of different interferometers in use today, but we will show only a couple for illustration purposes. Figure 2 shows a Twyman-Green interferometer that is commonly used to measure the flatness of a sample, called the test mirror in the figure.[7] The resulting interference pattern gives information on how this mirror differs from a perfectly flat mirror. A sample could be measured in transmission by placing it in front of the test mirror so the beam passes twice through the sample. A sample could be tested in single pass by using an interferometer such as the Mach-Zehnder shown in Figure 3.

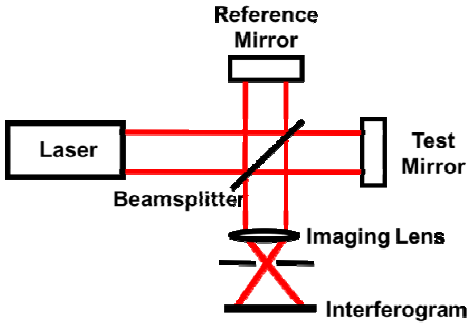


Figure 2. Twyman-Green interferometer.

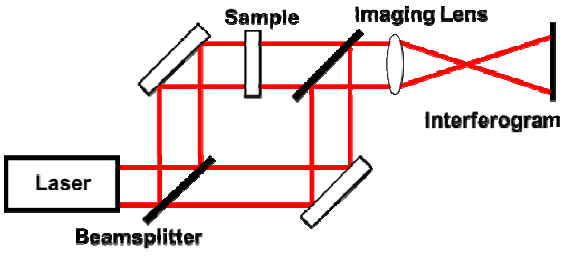


Figure 3. Mach-Zehnder interferometer.

Instead of measuring the surface shape or the optical thickness of the sample it is sometimes convenient to measure the surface slope or gradient of the optical thickness. Interferometers that measure slope are called shearing or differential interferometers. There are many examples of shearing interferometer interferometers, but perhaps the most famous is the Nomarski interferometer (Differential interference contrast, DIC) shown in Figure 4a.[6] In this case, polarization techniques are used to form two laterally displaced images of the surface under test with the result that we are measuring surface slope in the direction of the lateral displacement (shear) of the sample. If we wanted to measure a thin sample in transmission, and a double pass measurement of the sample was acceptable, the sample shown in the figure could be replaced with the transmission sample and a mirror. A sample could be measured in single pass using the Nomarski interferometer shown in Figure 4b.

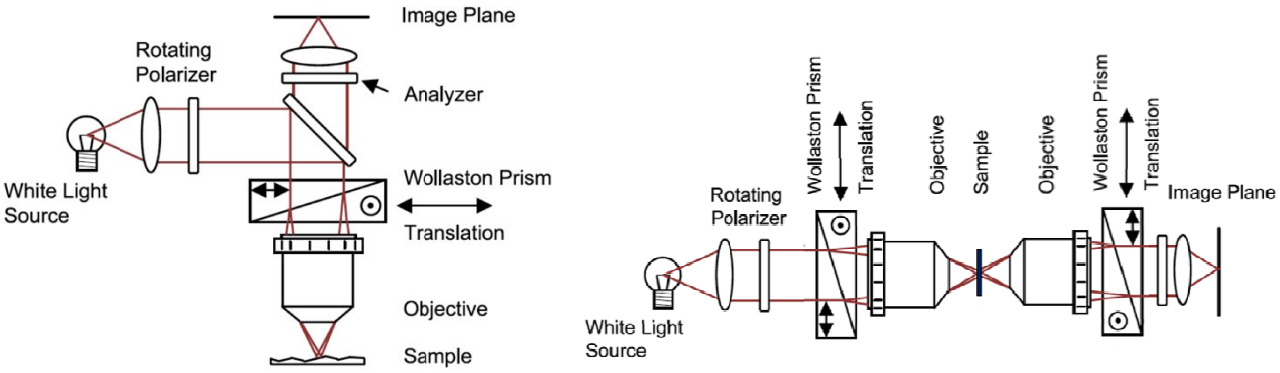


a) Reflection measurements b) Transmission measurements

Figure 4. Nomarski interferometer – Differential Interference Contrast (DIC)

Since the lateral shear interferometer is measuring the wavefront slope in only the direction of shear, two or more measurements with the shear in different directions, preferably orthogonal directions, are required to determine the wavefront being measured. Fortunately, there are several interferometers that can simultaneously measure the slope in two orthogonal directions. [8-10]

While there are hundreds of other two beam interferometers, their fundamental properties do not differ much from the examples shown above.

## 3. TECHNIQUES FOR GETTING INTERFEROMETRIC DATA INTO A COMPUTER

To get the most out of an interferometric measurement, the data has to be analyzed using a computer. There are several techniques for getting interferometric data into a computer.

### 3.1 Phase-shifting interferometry (PSI)

Many computerized interferometers use a technique called phase-shifting because the phase-shifting technique provides a highly accurate, rapid way of getting the interferogram information into a computer and the inherent noise in the data taking process is so low that in a good environment angstrom or sub-angstrom optical path differences can be measured. While the earliest reference to PSI is believed to be 1966[11], the development and demonstration of PSI began in the 1970's[8, 12-14]. In PSI the phase difference between the interfering beams is either changed in discrete steps (sometimes called phase-stepping interferometry) or it is changed at a constant rate as the detector is read out[14]. It can be shown that by making three or more measurements of the irradiance of the interference pattern as the phase difference is varied, it is possible to accurately determine the phase difference between the two interfering beams. The most commonly used phase shift between consecutive frames of data is 90 degrees because it simplifies the calculations. Generally, more than three phase shifts are used to reduce the requirement for the phase shift being exactly 90 degrees[15].

The irradiance of the interference pattern can be written as

$$I(x,y) = I_{dc} + I_{ac}Cos[\phi(x,y) + \alpha(t)]$$

where $\phi(x,y)$ is the phase being measured and $\alpha(t)$ is the phase shift. If four frames of data are taken as the phase changes by 90° between readouts, the irradiance for the four measurements and the measured phase, $\phi(x,y)$, are given by

$$I_1(x,y) = I_{dc} + I_{ac}Cos[\phi(x,y)] \qquad if\ \alpha(t) = 0$$

$$I_2(x,y) = I_{dc} - I_{ac}Sin[\phi(x,y)] \qquad if\ \alpha(t) = \frac{\pi}{2}$$

$$I_3(x,y) = I_{dc} - I_{ac}Cos[\phi(x,y)] \qquad if\ \alpha(t) = \pi$$

$$I_4(x,y) = I_{dc} + I_{ac}Sin[\phi(x,y)] \qquad if\ \alpha(t) = \frac{3\pi}{2}$$

$$Tan[\phi(x,y)] = \frac{I_4(x,y) - I_2(x,y)}{I_1(x,y) - I_3(x,y)}$$

While this is a very simple equation, it is very powerful and an excellent way of getting interferogram data into a computer. As a result of the subtraction and division and performing the calculation at each detector point, the effects of fixed pattern noise and gain variations across the detector are canceled out, as long as the effects are not so large that the dynamic range of the detector becomes too small to be of use.

It is interesting to note that when the original ideas for PSI were developed, PSI was not practical. Solid-state detector arrays were not yet available, computers were large, expensive and not as powerful as you would want, and the required electronics were massive. The early phase-shifting interferometers built in the late 1960's and early 1970's were extremely expensive and difficult to build and they had racks of electronics and only a few discrete detectors, while presently PSI systems are built using inexpensive personal computers and 4 million pixels, or larger, detector arrays are common.

As an example of a phase-shifting interferometer we will show a computerized interferometric microscope system for the measurement of surface microstructure where a repeatability of the surface height measurements of less than 0.1 nm can be obtained for smooth surfaces and by using multiple-wavelengths and coherence scanning techniques surfaces having height variations larger than hundreds of microns can be measured to within an accuracy of a few nanometers.

Figure 5 shows a simplified schematic of the instrument[16-18], as well as a photo of a phase-shifting interference microscope. The configuration shown in the figure utilizes a two-beam Mirau interferometer at the microscope objective. In the figure a tungsten halogen lamp is used as the light source, although LEDs are currently more common. In the phase-shifting mode of operation, a spectral filter of approximately 40 nm bandwidth centered at 650 nm is used to increase the coherence length. For the vertical scanning mode of operation described below, the spectral filter is not used. Light reflected from the test surface interferes with light reflected from the reference. The resulting interference pattern is imaged onto the CCD array. The output of the CCD is digitized and read by the computer. The Mirau interferometer is mounted on either a piezoelectric transducer (PZT) or a motorized stage so that it can be moved vertically. Thus, a phase shift is introduced into one arm of the interferometer. By introducing a phase shift into only one arm while recording the interference pattern that is produced, it is possible to perform either the phase-shifting technique described above or the vertical scanning coherence sensing technique described below.

A typical result for measuring a sample, in this case a diamond turned mirror, is shown in Figure 6. On smooth surfaces, the measurement rms repeatability can be less than 0.1 nm.

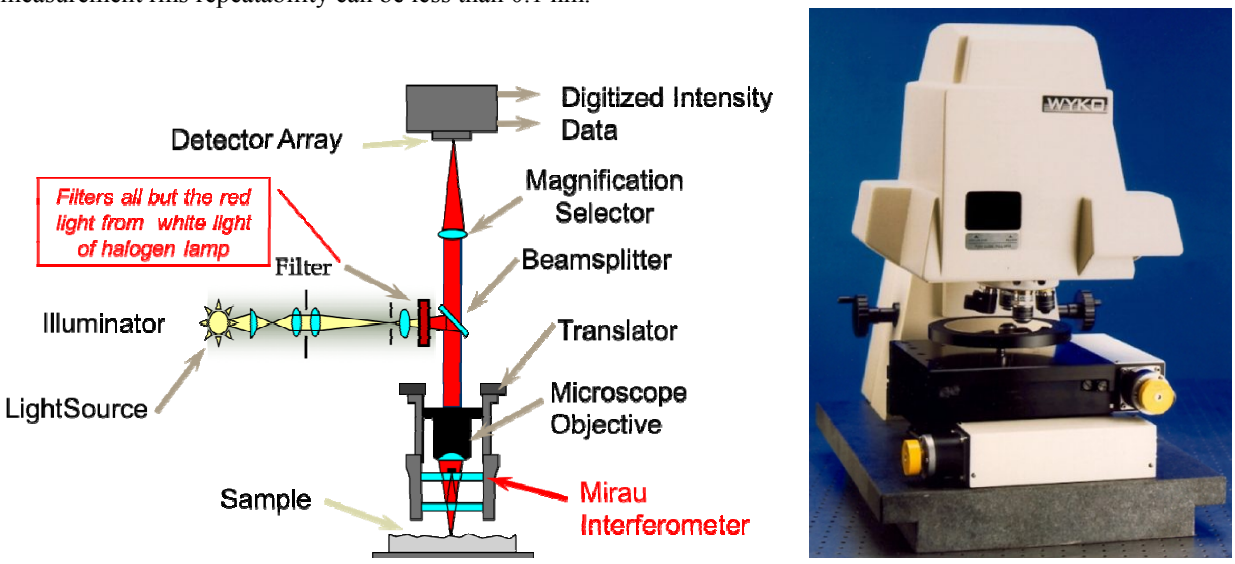


Figure 5. Phase-shifting interference microscope.

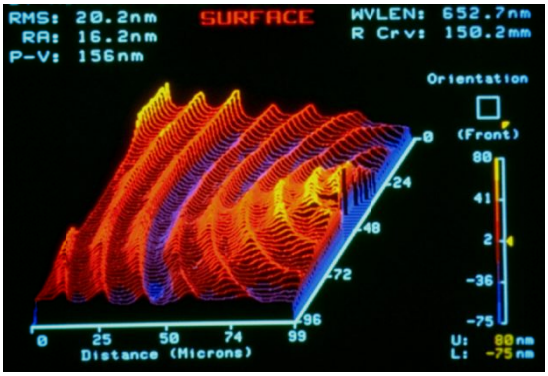


Figure 6. Measurement of diamond turned mirror.

In the phase-shifting mode of operation the phase is obtained by calculating the arc tangent that gives the phase modulo $2\pi$ and hence there may be discontinuities present in the calculated phase.[19] These $2\pi$ discontinuities can be removed as long as the slopes on the sample being measured are limited so that the actual phase difference between adjacent pixels is less than $\pi$ (surface height must change by less than a quarter-wavelength). The dynamic range can be increased by performing the measurement at two or more wavelengths[20-22].

In two-wavelength interferometry phase measurements are performed at two different wavelengths, and the two phase measurements are subtracted. Assuming no chromatic aberration is present, the result is equivalent to performing a single wavelength measurement at a longer equivalent wavelength given by the product of the two wavelength divided by the difference. This can be seen as follows.

$$phase\lambda_2 - phase\lambda_1 = 2\pi\left(\frac{1}{\lambda_2} - \frac{1}{\lambda_1}\right)OPD = \frac{2\pi}{\lambda_{eq}}OPD, \quad where$$

$$\lambda_{eq} = \frac{\lambda_2 \lambda_1}{Abs[\lambda_2 - \lambda_1]}$$

The maximum surface slope that can be measured is still a quarter-wavelength between adjacent detector points, but now it is a quarter of the equivalent wavelength, not a quarter of the individual shorter wavelengths. Thus, the dynamic range of the measurement is increased by the ratio of the equivalent wavelength to the individual single wavelength. Unfortunately, the noise is increased by the same ratio. It is easy to get around this increased noise when steps are being measured. The single wavelength measurements are correct, except the step heights are off by an integer number of half wavelengths. The errors in the step heights can be corrected by comparing the heights measured using the equivalent wavelength with the heights measured using the single wavelength and adding or subtracting an integer number of half wavelengths to the heights measured using the single wavelength so the difference between the single wavelength measurement and the equivalent wavelength measurement is less than a quarter wave. In this way it is possible to obtain the dynamic range of the equivalent wavelength and the accuracy of the single wavelength measurement.

Often, a better way to increase the dynamic range of an interference microscope is to use coherence scanning[23-25]. In the coherence scanning mode of operation a broad bandwidth source is used. Due to the large spectral bandwidth of the source, the coherence length of the source is short, and good contrast fringes will be obtained only when the two paths of the interferometer are closely matched in length. Thus, if in the interference microscope the path length of the sample arm of the interferometer is varied, the height variations across the sample can be determined by looking at the scan position for each sample point for which the fringe contrast is a maximum. In this measurement there are no height ambiguities and since in a properly adjusted interferometer the sample is in focus when the maximum fringe contrast is obtained, there are no focus errors in the measurement of surface microstructure. In the vertical scanning mode, nearly any type of surface can be measured as long as the reflected light gets back through the microscope objective. However, care has to be taken that while almost any surface can be measured, there may be errors in the measurement. For example, if a very rough surface is measured, there may be multiple reflections of the light in the surface structure resulting in errors in the surface measurement[26-27]. In spite of this potential problem, the coherence scanning interference microscope is widely used in a wide variety of industries including magnetic data storage, semiconductor, machine tool, biomedical, etc.

It is interesting that the ideas of coherence scanning certainly go back to the days of Michelson, but it was not until the 1990's that the required detectors and computers were available for making a practical commercial system[25]. The early commercial systems used DSPs to perform the required calculations to simultaneously determine the coherence calculations at all detector points. Then personal computers became powerful enough to do the calculations without DSPs and since then as computers became faster and faster it became easier to do the calculations at a million or more data points at vertical scan speeds of greater than 25 microns per second. It is interesting to think about what Michelson could have done if he had the computers, electronics, and detectors that we now have.

Temporal phase-shifting interferometry is extremely useful, but sometimes either the sample or the environment is changing so fast there is need for taking all the phase-shifting frames in a single shot. A single-shot interferometer is less insensitive to vibration and if a sample is changing with time, the changes in the sample can be measured and movies can be made showing how the sample changes as a function of time. In temporal phase shifting interferometry we are taking three or more frames of data at different time, while in the single-shot measurement all the data is taken at once, however there is a time-space tradeoff. In the single shot approach more detector elements are required to get the same spatial resolution. Fortunately, detector arrays having millions of pixels are now available.

### 3.2 Spatial carrier

One of the oldest single-shot technique is what is often called the spatial carrier technique.[28-30] In the spatial carrier technique, a lot of tilt is introduced between the two interfering beams so a lot of tilt fringes are obtained as show in Figure 7. Because of the tilt fringes the resulting interferogram is sometimes called a hologram. A Fourier Transform can be taken of the hologram to give different orders as also shown in Figure 7. The first order can be spatially filtered out and an inverse Fourier transform can be taken to obtain the wavefront. When the technique was first introduced, it was not very useful because detector arrays having a large number of pixels were not available. Now that solid-state detector

arrays having several million pixels are available and computers that can rapidly perform Fast-Fourier transforms are readily available, the spatial carrier approach has become extremely useful. Two possible drawbacks to the system are that the large number of interference fringes requires increased source coherence requirements and the large tilt between the two interfering beams may limit the accuracy of the measurement, however the technique is widely used and extremely useful.

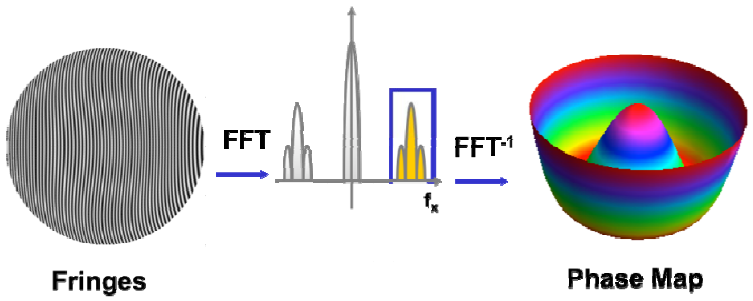


Figure 7. Spatial carrier technique for obtaining interferometric data in a single shot.

A second way of analyzing the spatial carrier interferogram is to adjust the tilt so there are approximately four detector elements between adjacent interference fringes. In this way we could get the four phase shifted frames by looking at the signals coming from four adjacent detector pixels. While this approach works perfectly only if the wavefront being measured is a perfect plane wave, it turns out it still works quite well when we are measuring non-plane waves and a system using this approach is shown in Figure 8. Instead of using a 2 x 2 array of pixels to get the 4 phase shifted pixels, it is often better to use a 3 x 3 array, as shown in the figure, to get the phase shifted data points. This reduces the sensitivity to the tilt being just right to get 90-degree phase differences, but it does slightly decrease the spatial resolution.

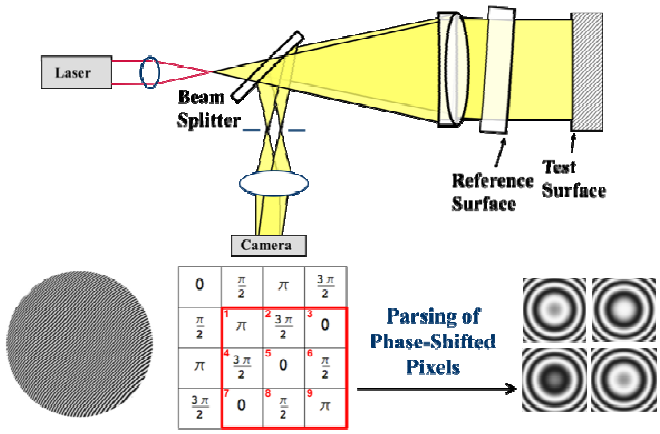


Figure 8. Measurement of diamond turned mirror.

### 3.3 Single-shot holographic polarization dynamic interferometer

Another approach is to have all four phase-shifted frames fall on a single CCD camera as shown in Figure 9. In this arrangement, an interferometer is used where a polarization beamsplitter causes the reference and test beams to have orthogonal polarization. After the two orthogonally polarized beams are combined they pass through a holographic element that splits the beam into four separate beams resulting in four interferograms. These four beams pass through a birefringent mask that is placed just in front of a CCD camera. The four segments of the birefringent mask introduce

phase shifts between the test and reference beams of 0, 90, 180, and 270 degrees. A polarizer with its transmission axis at 45 degrees to the direction of the polarization of the test and reference beams is placed after the phase masks just before the CCD array. Thus, all four phase-shifted interferograms are detected in a single shot on a single detector array.[31]

This technique works extremely well as long as a single wavelength is being used. However, if the source wavelength changes the holographic element diffracts the light at different angles and the four phase shifted frames are not at the right location on the detector. A better approach that works well with different wavelengths, including white light, is the pixelated polarizer array described next.

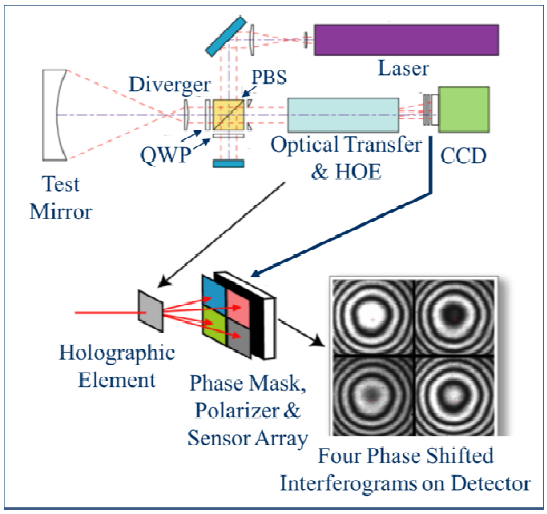


Figure 9. Single-shot holographic polarization dynamic interferometer.

### 3.4 Pixelated polarizer array interferometer

A phase-shifting technique that works well with multiple wavelengths, or even white light, involves the use of a quarter waveplate followed by linear polarizers at different angles.[32-34] For this technique, the phase shift between the two interfering beams is nearly independent of wavelength. The quarter waveplate is oriented to convert one of the two interfering beams into left-handed circular polarization and the other interfering beam into right-handed circular polarization. It can be shown that if these circularly polarized beams are transmitted through a linear polarizer, a phase-shift between the two interfering beams proportional to twice the rotation angle of the polarizer results[35]. See Figure 10.

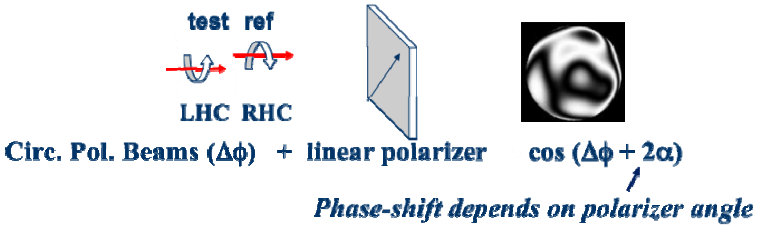


Figure 10. Use of polarizer as phase shifter.

Thus, if a phase mask is made of an array of 4 linear wire-grid polarizer elements having their transmission axes at 0, 45, 90, and 135 degrees as shown in Figure 11, where a polarizer element is placed over each detector element, the mask will produce an array of four 0, $\pi/2$, $\pi$, and $3\pi/2$ degrees phase shifted interferograms. The size of the polarizer elements must be equal to the size of the pixels making up the detector array. This spatial phase-shifting technique does slightly

reduce the spatial resolution of the interferometer, but the effect on the spatial transfer function is small.[36] It is interesting to note that while it has been known for a long time that rotating a polarizer in a circularly polarized beam changes the phase of the beam, it is only within the past few years that it is possible to produce the required wire-grid polarizer array to work in the visible spectrum.

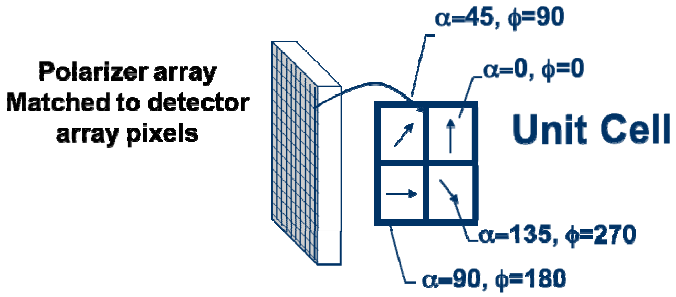


Figure 11. Polarizer array matched to detector array pixels.

Figure 12 shows one possible arrangement of a Twyman-Green interferometer using the micropolarizer phase-shifting array. The essential characteristics of the two-beam interferometer are that the test and reference beams have orthogonal polarization and the size of the micropolarizer array matches the CCD array. In the figure the polarization beam splitter (PBS) sends one state of polarization to the reference arm and the orthogonal state to the test arm. A quarter-wave plate (QWP) is placed in each arm and after the light passes through each QWP twice the direction of polarization is rotated 90-degrees and the beam that was reflected by the PBS on the first pass will be transmitted on the second pass and the beam that was transmitted on the first pass will be reflected on the second pass. The QWP placed in the output beam converts the orthogonally polarized test and reference beams into left-handed and right-handed circularly polarized beams.

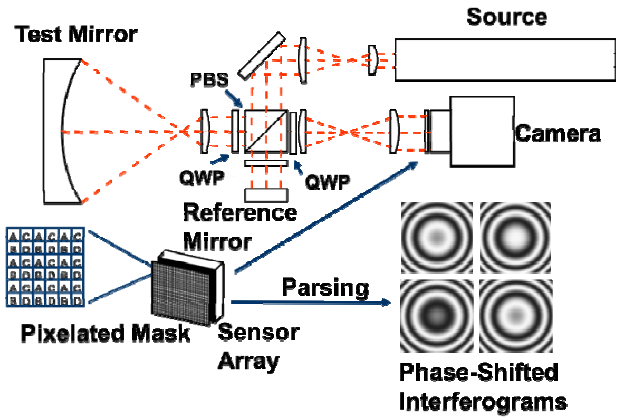


Figure 12.Twyman Green interferometer using the micropolarizer phase-shifting array.

Using this interferometer, it is possible to have the optics under test and the interferometer on different tables without any vibration isolation. By averaging several frames of data the effects of air turbulence can be minimized. If a surface is vibrating it is possible to determine precisely how the surface is vibrating. Movies can be made showing how the shape of the vibrating surface is changing in time. Figure 13 shows one frame of data from a movie made of a disk vibrating at a frequency of 3069 Hz.

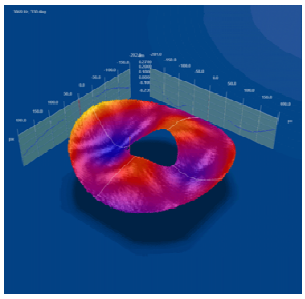

Figure 13. One frame of data from a movie made of a disk vibrating at a frequency of 3069 Hz.

The micropolarizer array can also be used with many other types of interferometers, including a Fizeau interferometer.[37] It also works very well with broadband white light sources and can be used in a very low coherence interferometer which will give low coherence noise (no spurious fringes from unwanted reflections).

## 4. INTERFEROMETRIC MEASUREMENT OF CELLS AND TISSUE

The techniques described above that are widely used in metrology are now being used for looking at cells and tissues. Figure 14 shows an example double pass measurement of live NIH 3T3 mouse fibroblast cells observed using a phase-shifting interference microscope similar to the one shown in Figure 5.[38] The pixelated polarizer array interferometer described above has been used to looking for looking at many biomedical/biological samples including samples of breast cancer cells and rat cardiac myocytes. The specific interferometer used is the Linnik interference microscope shown in Figure 15. Figure 16 shows some results for looking at the breast cancer cells and Figure 17 shows one frame of a video made of beating rat cardiac myocytes.

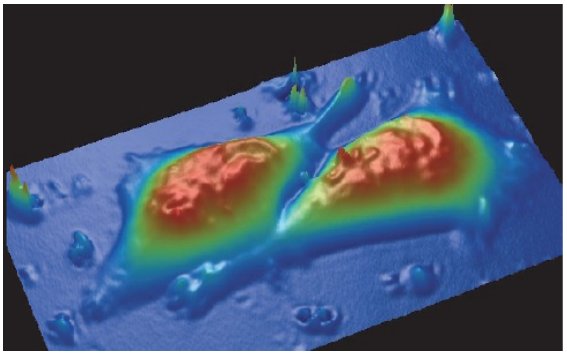

Figure 14. Live NIH 3T3 mouse fibroblast cells observed by the optical profiler.[38]

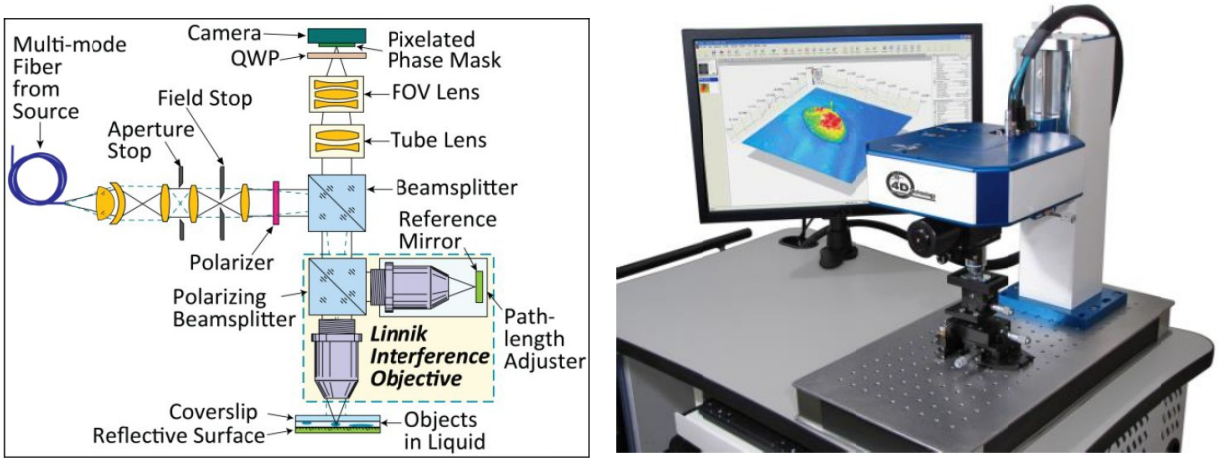


Figure 15. Linnik interference microscope schematic and photograph.[39-42]

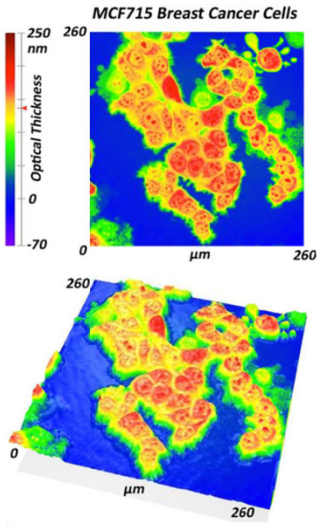


Figure 16. Breast cancer cells.[41]

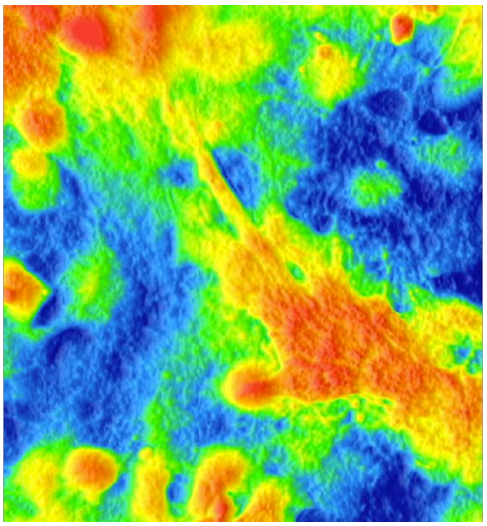

Figure 17. One frame of a 15 fps video made of beating rat cardiac myocytes.

Many other examples of interferometric measurements of cells and tissues can be found in the excellent book given in reference 43.

## 5. CONCLUDING REMARKS

Now is a very exciting time in the area of interferometric measurement of cells and tissues and the resulting analysis of the measurement results. By using measurement techniques developed over the years for metrology applications, as well as some new techniques that will surely be developed, the use of modern detectors, light sources, and computers and great new software, the potential for determining new properties of biomedical/biological samples is almost unlimited.

## 6. ACKNOWLEDGMENTS

The author wishes to acknowledge many useful conversations with Katherine Creath concerning the material in this paper.

## REFERENCES


[1] Born, M. and Wolf, E., [Principles of Optics], Cambridge University Press, Cambridge & New York, (1999).
[2] Hecht, E., [Optics], Addison Wesley, Reading, MA, (2016).
[3] Hariharan, P., [Basics of Interferometry], Academic Press, Burlington, MA, (2010).
[4] Francon, M., [Optical Interferometry], Academic Press, New York, (1966).
[5] Steel, W. H., [Interferometry], Cambridge University Press, Cambridge, (1983).
[6] Francon, M. and Mallick, S., [Polarization Interferometers], Wiley-Interscience, New York, (1971).
[7] Malacara, D. Ed., [Optical Shop Testing], Wiley-Interscience, New York, (2007).
[8] Wyant, J. C., "Double Frequency Grating Lateral Shear Interferometer," Appl. Opt. 12, 2057-2060 (1973).
[9] Primot, J., "Three-wave lateral shearing interferometer," Appl. Opt. 32, 6242-6249 (1993).
[10] Chanteloup, J., "Multiple-wave lateral shearing interferometry for wave-front sensing," Appl. Opt. 44, 1559-1571 (2005).
[11] Carré, P., "Installation et utilisation du comparateur photoelectrigue et Interferentiel du Bureau International de Poids et Measures," Metrologia (2)1, 13-23 (1966).
[12] Crane R., "Interference Phase Measurement," Appl. Opt. 8, 538-542 (1969).
[13] Bruning, J. H., Herriott, D. R., Gallagher, J. E., Rosenfeld, A. D. White, D. P. and Brangaccio, D. J. "Digital Wavefront Measuring Interferometer for Testing Optical Surfaces and Lenses," Appl. Opt. **13**, 2693-2703 (1974).
[14] Wyant, J. C. "Use of an ac heterodyne lateral shear interferometer with real-time wavefront correction systems," Appl. Opt. 14, 2622-2626, (1975).
[15] Schwider, J., Burow, R., Elssner, K. E., Grzanna, J., Spolaczyk R., and Merkel, K., "Digital wave-front measuring interferometry: Some Systematic Error Sources," Appl. Opt. 22, 3421-3432 (1983).
[16] Bhushan, B., Wyant, J. C., and Koliopoulos, C.L., "Measurement of surface topography of magnetic tapes by Mirau interferometry," Appl. Opt. 28, 1489-1497, (1985).
[17] Wyant, J. C., "Optical profilers for surface roughness", Proc. SPIE 525, 174-180, (1985).
[18] Wyant, J. C. and Creath, K. "Advances in Interferometric Optical Profiling," Int. J. Mach. Tools Manufact. 32, No.1/2, 5-10 (1992).
[19] Ghiglia, D. and Pritt, M., [Two-Dimensional Phase Unwrapping: Theory, Algorithms, and Software], Wiley-Interscience, New York, (1998).
[20] U.S. Patent No. 4,832,489 "Two-wavelength phase-shifting interferometer and method," James C. Wyant and K. Creath, 1989.
[21] Cheng, Yeou-Yen and Wyant, J. C., "Two-wavelength phase shifting interferometry," Appl. Opt. 23, 4539-4543 (1984).
[22] Cheng, Yeou-Yen and Wyant, J. C., "Multiple-wavelength phase-shifting interferometry," Appl. Opt. 24, 804-807 (1985).
[23] Davidson, M., Kaufman, K., Mazor, I., and Cohen, F., "An Application of Interference Microscopy to Integrated Circuit Inspection and Metrology," Proc. SPIE 775, 233-247 (1987).
[24] Dresel, T., Hausler, G., and Venzke, H., "Three-dimensional sensing of rough surfaces by coherence radar," Appl. Opt. 31, 919-925 (1992).
[25] Caber, P. J., "An Interferometric Profiler for Rough Surfaces," Appl. Opt. 32, 3438-3441 (1993).
[26] Gao, F., Leach, R. K., Petzing, J., and Coupland, J. M. , "Surface measurement errors using commercial scanning white light interferometers," Meas. Sci. Technol. 19 015303 (2008).
[27] Leach, R. K., Giusca, C. L., and Coupland, J. M., "Advances in calibration methods for micro- and nanoscale surfaces," Proc. SPIE 8430, 84300H (2012).
[28] Takeda M., Ina, H., and Kabayashi, S., "Fourier-Transform Method of Fringe-Pattern Analysis for Computer-Based Topography and Interferometry," J. Opt. Soc. Am., **72**, 156-160 (1982).
[29] Womack K. H., "Interferometric Phase Measurement Using Spatial Synchronous Detection," Proc. SPIE, **429**, 8-15 (1983).
[30] Takeda M., Gu, Q., Kinoshita, M., Takai, H., and Takahashi, Y., "Frequency-Multiplex Fourier-Transform Profilometry: A Single Shot Three-Dimensional Shape Measurement of Objects with Large Height Discontinuities and/or Surface Isolations," Appl. Opt., 36, 5347-5354 (1997).
[31] U. S. Patent 6,304,330, "Methods and apparatus for splitting, imaging, and measuring wavefronts in interferometry," James E. Millerd and Neal J. Brock, (2001).

[32] Millerd J., N. Brock, J. Hayes, M. North-Morris, M. Novak and J. C. Wyant, “Pixelated Phase-Mask Dynamic Interferometer,” Proc. SPIE, 5531, 304-314 (2004).
[33] Novak M., Millerd, J., Brock, N., North-Morris, M., Hayes J., and Wyant, J. C., “Analysis of a Micropolarizer Array-Based Simultaneous Phase-Shifting Interferometer,” Appl. Opt., **44**, 6661-6868 (2005).
[34] Brock, N., Hayes, J., Kimbrough, B., Millerd, J., North-Morris, M., Novak M., and Wyant, J. C., “Dynamic Interferometry,” Proc. SPIE 5875, 58750F, (2005).
[35] Suja Helen, S., Kothiyal, M.P., and Sirohi, R.S., "Achromatic phase-shifting by a rotating polarizer", Opt. Comm. 154, 249 (1998).
[36] Kimbrough B., and Millerd, J., “The spatial frequency response and resolution limitations of pixelated mask spatial carrier based phase shifting interferometry,” Proc. SPIE 7790, (2010).
[37] Kimbrough, B., Millerd, J., Wyant, J., and Hayes, J., “Low coherence vibration insensitive Fizeau interferometer,” Proc. SPIE 6292, 62920F, (2006).
[38] Schmit, J., Reed, J., Novak, E., and Gimzewski, J. K., "Performance advances in interferometric optical profilers for imaging and testing," J Opt A-Pure and Applied Optics 10(6), 064001 (2008)
[39] Creath, K. (2010). "Dynamic quantitative phase images of pond life, insect wings, and in vitro cell cultures." Proc. SPIE 7782: 77820B.77801-77813.
[40] Creath, K. and G. Goldstein (2012). "Dynamic quantitative phase imaging for biological objects using a pixelated phase mask." Biomedical Optics Express 3(9): 2866-2880.
[41] Creath, K. and G. Goldstein (2013). "Processing and improvements in dynamic quantitative phase microscope." Proc. SPIE 8589: 85891A.
[42] Goldstein, G. and K. Creath (2014). "Quantitative Phase Microscopy: How to make data meaningful." Proc. SPIE 8949: 89491C.
[43] Popescu, G., [Quantitative Phase Imaging of Cells and Tissues], McGraw-Hill, New York, (2011).